Ionization and dissociation of CH_3I in intense laser field

Hongtao Liu, Zheng Yang, and Zhen Gao
State Key Laboratory of Molecular Reaction Dynamics, Center of Molecular Science, Institute of Chemistry, Chinese Academy of Sciences, Bejing 100080, People's Republic of China

Zichao Tang[a)]
State Key Laboratory of Molecular Reaction Dynamics, Center of Molecular Science, Institute of Chemistry, Chinese Academy of Sciences, Bejing 100080, People's Republic of China and State Key Laboratory of Molecular Reaction Dynamics, Dalian Institute of Chemical Physics, Chinese Academy of Sciences, Dalian 116023, People's Republic of China

(Received 21 July 2006; accepted 28 November 2006; published online 31 January 2007)

The ionization-dissociation of methyl iodide in intense laser field has been studied using a reflection time-of-flight mass spectrometry (RTOF-MS), at a laser intensity of $\leqslant 6.6\times10^{14}$ W/cm^2, $\lambda=798$ nm, and a pulse width of 180 fs. With the high resolution of RTOF-MS, the fragment ions with the same M/z but from different dissociation channels are resolved in the mass spectra, and the kinetic energy releases (KERs) of the fragment ions such as I^{q+} ($q=1-6$), CH_m^+ ($m=0-3$), C^{2+}, and C^{3+} are measured. It is found that the KERs of the fragment ions are independent of the laser intensity. The fragments CH_3^+ and I^+ with very low KERs (<1 eV for CH_3^+ and <0.07 eV for I^+) are assigned to be produced by the multiphoton dissociation of CH_3I^+. For the fragments CH_3^+ and I^+ from CH_3I^{2+}, they are produced by the Coulomb explosion of CH_3I^{2+} with the interaction from the covalent force of the remaining valence electrons. The split of the KER of the fragments produced from CH_3I^{2+} dissociation is observed experimentally and explained with the energy split of $I^+(^3P_2)$ and $I^+(^3P_{0,1})$. The dissociation $CH_3I^{3+}\rightarrow CH_3^++I^{2+}$ is caused by Coulomb explosion. The valid charge distance R_c between I^{2+} and CH_3^+, at which enhanced ionization of methyl iodide occurs, is obtained to be 3.7 Å by the measurements of the KERs of the fragments CH_3^+ and I^{2+}. For the CH_3I^{n+} ($n\geqslant 3$), the KERs of the fragment ions CH_3^{p+} and I^{q+} are attributed to the Coulomb repulsion between CH_3^{p+} and I^{q+} from $R_c\approx 3.7$ Å. The dissociation of the fragment CH_3^+ is also discussed. By the enhanced ionization mechanism and using the measured KER of I^{q+}, all the possible Coulomb explosion channels are identified. By comparing the abundance of fragment ions in mass spectrum, it is found that the asymmetric dissociation channels with more charges on iodine, $q>p$, are the dominant channels. © *2007 American Institute of Physics*. [DOI: 10.1063/1.2424703]

I. INTRODUCTION

The dynamics of molecules in an intense laser field has remained a hot topic and has been extensively studied in the past decades.[1–3] But the understanding of the molecular dynamics in an intense laser field is obtained only for small molecules, especially for diatomic molecules.[4,5] Niikura *et al.* studied the dynamics of nonsequential double ionization of H_2 and observed the electron recollision at a sub-laser-cycle.[6] Theoretical and experimental results indicated that the laser-induced Coulomb explosion of diatomic molecule occurred at a critical internuclear distance R_c, at which enhanced ionization processes happened.[7–12] However, in the case of ionization-dissociation of polyatomic molecules involved in laser intensities with an intermediate range ($10^{13}-10^{15}$ W/cm^2), the situation is much complicated and many fundamental questions still remain unanswered.[13]

Methyl iodide, as one of the simplest alkyl halides, was used extensively in the study of photodissociation.[14–18] The experimental results showed that the photoexcitation of the CH_3I and CH_3I^+ reached the dissociative A band firstly, then the C–I bond of methyl iodide was broken to produce CH_3 (or CH_3^+) and I (or I^+) fragments. With the advent of the picosecond and femtosecond lasers, the examinations of the real time dynamics of the photodissociation event become possible. Using femtosecond time-resolved mass spectrometry, Zhong *et al.*[19,20] studied the CH_3I dissociation by the kinetic-energy-resolved time of flight mass spectrometry (TOF-MS) and measured the dissociation time of CH_3I to be about 150 fs. It is known that the dissociation of CH_3I followed by the ionization of neutral fragments (ladder switching) is the dominant process in a weak laser field with a longer pulse duration (approximately nanoseconds). But in an intense laser field with a shorter pulse duration (picosecond or femtosecond), the mechanism of multielectron dissociative ionization (MEDI) is used to explain most of the experimentally detected fragment ions of CH_3I produced by Coulomb explosion. Recently, Graham *et al.*[21] studied the angular distributions of fragment ions generated from the Coulomb explosion of methyl iodide ions with 50 fs intense laser pulse (10^{16} W/cm^2). Multiply charged iodine fragment ions (up to I^{7+}) were detected and the kinetic energy releases (KERs) of the I^{n+} were measured, but the detailed assignments of the dissociation channels were not given. Siozos

[a)]Electronic mail: zctang@dicp.ac.cn

et al.[22] studied the MEDI process of CH_3I in a strong picosecond laser field (10^{15} W/cm^2), and found that the KERs of the I^{n+} ions were much lower than those obtained by an intense femtosecond laser. So they suggested that the high charged I^{n+} ions ($n \geqslant 3$) in the picosecond laser field were produced from the further ionization of low charged I^+ and I^{2+} ions in the early part of the laser pulse. Later, the same group reported their new results of CH_3I in the intense picosecond laser field, with improved resolution of the time-of-flight (TOF) mass spectrometer.[23] They assigned some Coulomb explosion channels and measured the KERs of CH_3^+ ions from different channels, while no reports about the assignments of H^+, C^{n+}, CH^+, and CH_2^+ fragments generated by the Coulomb explosion of CH_3I in the intense laser field have been found.

The alignment of CH_3I molecule in the intense laser field was found to depend on the durations of laser pulse. CH_3I molecule can dynamically align in the intense picosecond laser field[23] but cannot dynamically align in the intense femtosecond laser field.[21,24] The different situations were explained by the large moment of inertia and long rotational period ($\sim$1 ps) of CH_3I. The alignment of CH_3I along the direction of the laser field within a scale of femtosecond laser pulse was though to be impossible. The anisotropy of the measured fragment ions is due to an angle-dependent ionization-dissociation. This is similar to the case of some diatomic molecules (I_2 and N_2) where the ionization-dissociation has a maximum rate when the molecular axis is parallel to the laser E field.[25] When the plane of the detector is perpendicular to the laser field, the observed ions are maximum. However, the detailed ionization-dissociation processes of methyl iodide remain unclear.

In this paper, we report our study on the ionization-dissociation of methyl iodide in an intense laser field of 180 fs and $\leqslant 6.6 \times 10^{14}$ W/cm^2, detected by a home-built reflection time-of-flight mass spectrometer (RTOF-MS). Based on the high resolution of our RTOF-MS, the KERs of the fragment ions are determined with high precision. It is found that both the multiphoton dissociation of CH_3I^+ and the Coulomb explosion of CH_3I^{n+} ($n > 1$) coexisted in the experiments. The sequential two-body separation or direct multiple fragmentations in the Coulomb explosion of CH_3I^{n+} are discussed. For the dissociation of CH_3I^{2+} in the intense laser field the contribution of the covalent force of the valence electrons is considered. The valid intercharge distance between the virtual CH_3^{p+} and I^{q+} is discussed and R_c is defined for methyl iodide. The enhanced ionization mechanism is used to explain the Coulomb explosion of CH_3I^{n+}. The laser intensity effect on the KERs of fragment ions is studied, and it is confirmed that the enhanced ionization of methyl iodide in the intense laser field really happened. Finally, by comparison of the abundance of different fragment ions in mass spectrum, the charge distributions of methyl iodide prior to the Coulomb explosion are discussed.

II. EXPERIMENT

The laser system used in this study is a mode-locked Ti:sapphire femtosecond laser with an oscillator (Coherent, Mira-seed) pumped by a cw second harmonic of a Nd:YVO_4 laser (Coherent, Verdi-5). As a seed pulse, the 798 nm laser pulse (80 fs) is stretched and led to an eight pass Ti:sapphire amplifier (Quantronix, Odin) which is pumped by the second harmonic of a neodymium-doped yttrium lithium fluoride laser (Quantronix, DPH-527) operating at 10 Hz. The amplified laser pulse then is switched to a parallel grating pair to be compressed back to the short pulse duration (180 fs). The energy of the amplified laser pulse can reach 0.5 mJ/pulse. The amplified laser beam is focused by a lens of $f=80$ mm and is led into the acceleration region in a home-built RTOF-MS. In front of the lens, a half wave plate is used to change the polarization direction of a linearly polarized laser pulse, or a $\lambda/4$ wave plate is used to produce a circularly polarized laser pulse. The intensity of the laser at the focus area is determined from the thresholds of charge states of Xe ionization[26,27] and from the calculation using the known pulse parameters. The four charged states of xenon observed in mass spectrum are consistent with the calculation. Different laser intensities are achieved by absorptive neutral density filters.

A detailed description of the RTOF-MS was given in our previous reports.[28,29] In this experiment, CH_3I (analytical reagent) was vaporized and seeded in helium (purity of 99.999%) in a vacuum stainless steel bottle (volume of about 2 cm^3) to yield a total pressure of 200 kPa. The calculation of CH_3I in the mixed gas was less than 0.1% in mole. The mixed gas passed through a pulsed valve supersonic expanded into the source chamber of RTOF-MS. After passing a skimmer (diameter of 1 mm), the mixed gas entered the reaction chamber, where it was intersected with the focused femtosecond laser beam to generate the ionization-dissociation. Following ionization-dissociation, the ions were accelerated with a dual stage electrostatic field to fly in the direction perpendicular to both the molecular beam and the laser beam. The ion products experienced two sets of deflectors and einzel lenses, and then were reflected by a reflector to reach the detector, a dual microchannel plate (MCP). The output signal from the MCP was recorded and analyzed by a digital oscilloscope (Tektronix TDS5052). The timing sequence of the pulsed valve and the laser shot was optimized by a digital delay pulse generator (Stanford Research DG535). Typically, the final digitized mass spectrum was obtained from the average of 1000 laser shots. The mass resolution of the mass spectrometer ($M/\Delta M$) is better than 2000, so the splits of the same mass peak caused by the Coulomb explosion can be resolved. The source chamber, the acceleration region, and the reflection region were all pumped with turbomolecular pumps. The corresponding operating pressures were 10^{-2}, 10^{-4}, and 10^{-5} Pa, respectively.

III. RESULTS AND DISCUSSION

A. Mass spectra

In Fig. 1 the mass spectra of the fragment ions produced from CH_3I at a laser intensity of 6.6×10^{14} W/cm^2 for (a) parallel laser polarization and (b) perpendicular laser polarization with respect to the TOF axis are presented. In both spectra, the prominent parent ion peak, the doubly charged

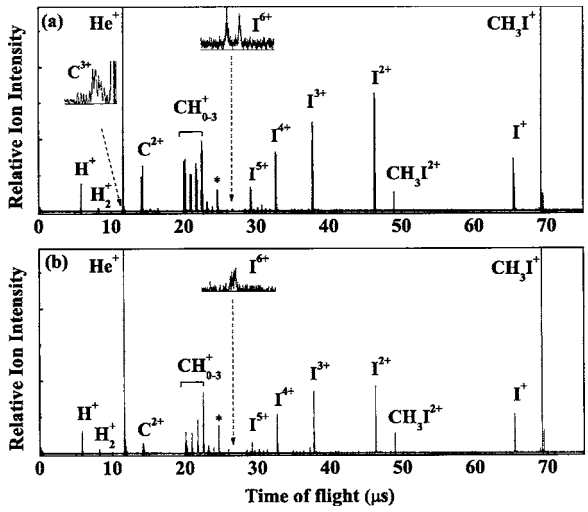

FIG. 1. Mass spectrum of CH_3I irradiated at a laser intensity of 6.6×10^{14} W/cm^2 with (a) laser polarization parallel to the TOF axis and (b) laser polarization perpendicular to the TOF axis.

parent ion peak, and the fragment ion peaks [such as I^{n+} $(n \leqslant 6)$, CH_m^+ $(m=0-3)$, C^{2+}, H_2^+, and H^+] are all recorded. The He^+ ions with very intense peaks produced from carrier gas are also presented. The peak denoted with asterisk originates from the residual water in the vacuum chamber. In Fig. 1(a), the C^{3+} ions from the Coulomb explosion are detected with weak peaks on one side of the He^+ peak, while at the other side of He^+, C^{3+} ion peaks are immersed due to the disturbance of the high frequency oscillation of the strong He^+ signals. The CH_3I^+ and CH_3I^{2+} peaks presented in Fig. 1 have no splits because these ions are only from the ionization of CH_3I. By measuring the full width at half maximum of the CH_3I^{2+} ion peak and the He^+ peak, the mass resolution $(M/\Delta M)$ of the RTOF-MS is obtained to be higher than 2000, and the corresponding energy resolution is better than 0.01 eV.

For polyatomic molecules, the Coulomb explosion can follow sequential two-body charge separation channels or nonsequential multiple fragmentation channels.[30,31] In the sequential two-body processes, there might be two dissociation patterns. One is as follows:

$$CH_3I^{n+} \rightarrow H^+ + [CH_2I]^{(n-1)+}, \tag{1a}$$

$$[CH_2I]^{(n-1)+} \rightarrow H^+ + [CHI]^{(n-2)+}, \tag{1b}$$

$$[CHI]^{(n-2)+} \rightarrow H^+ + [CI]^{(n-3)+}, \tag{1c}$$

$$[CH_2I]^{(n-1)+} \rightarrow [CH_2]^{(p-1)+} + I^{q+}, \tag{1d}$$

$$[CHI]^{(n-2)+} \rightarrow CH^{(p-2)+} + I^{q+} \quad (n=p+q). \tag{1e}$$

Because the fragment ions such as CH_2I^+, CHI^+, CH_2I^{2+}, CHI^{2+}, etc. are not observed in our experiments, all of the above dissociation channels are excluded. The other pattern is

$$CH_3I^{n+} \rightarrow CH_3^{p+} + I^{q+} \quad (n=p+q). \tag{2}$$

The fragment CH_3^{p+} ions can undergo sequential dissociations into smaller fragment ions. The observed CH_3^+ ions in the mass spectrum can only be produced from two-body channels, shown in channel (2), so channel (2) is a real dissociation channel in the experiments. In the nonsequential process with multiple fragmentations, methyl iodide ions can be dissociated as follows:

$$CH_3I^{n+} \rightarrow mH^+ + [CH_{3-m}]^{(p-m)+} + I^{q+} \quad (n=p+q). \tag{3}$$

Some high charged parent precursors are also possible to fragment directly through the Coulomb explosion via Eq. (3), which will be discussed in Sec. III B.

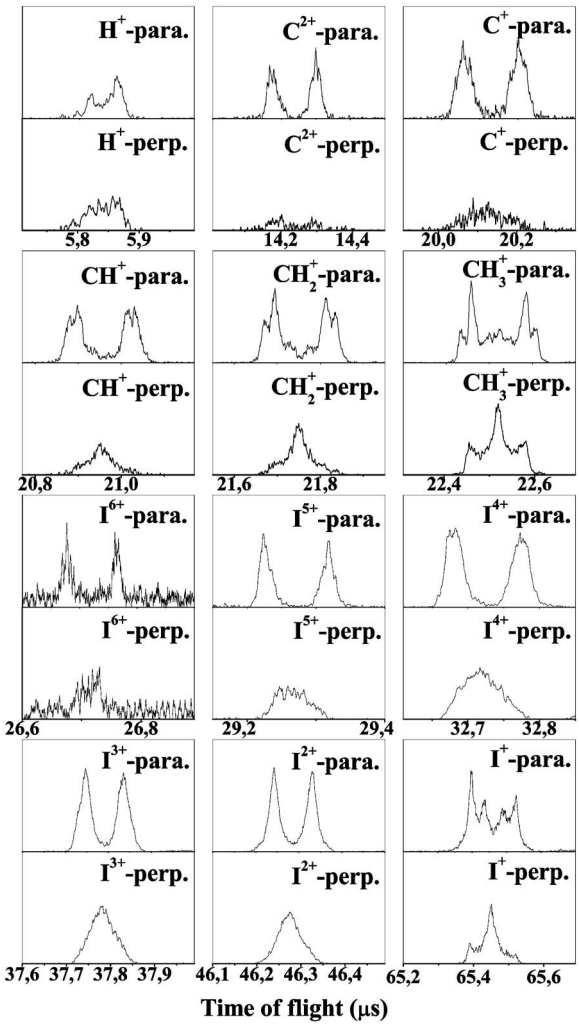

FIG. 2. The enlarged typical fragment ion peaks extracted from Fig. 1, which shows the difference between the CH_3I molecule at parallel laser polarization (upper) and perpendicular laser polarization (lower).

Figure 2 is the enlarged mass spectrum of typical ion peaks extracted from Fig. 1. For the case of parallel laser polarization, the mass peaks are intense and each mass peak profile exhibits a clear symmetrical double peak structure as a result of the KER of the fragment ions, while for the case of perpendicular laser polarization, the intensity of the mass peaks is lower and exhibits no symmetrical double peak structures. This prominent difference is due to the fact that the fragment ions have maximum distributions along the direction of laser polarization, and the ions with velocity around the TOF axis are energy resolved. In our experiment, the laser pulse used is 180 fs, much shorter than the rota-

tional period of CH_3I. So the results are similar to those reported by Ma *et al.*[24] That is, geometric alignment of molecules in the intense laser field is dominant and the dynamic alignment can be negligible. This conclusion has also been demonstrated in our experiments by the comparison of ionization-dissociation of CH_3I using circular and linear laser polarizations, respectively. It has been shown that the mass spectra obtained with circular and parallel laser polarizations have no substantial difference, indicating that the dynamic alignment of molecules in the intense laser field is not important.[32] Some detected fragment ions are much suppressed in the case of perpendicular laser polarization due to the limits of the acceptance angle of the detector. It can be seen clearly that C^+ and C^{2+} ions in Fig. 1(b) are much weaker than those in Fig. 1(a), and C^{3+} ions are observed in Fig. 1(a) but not in Fig. 1(b).

As shown in Fig. 2, when the laser polarization is perpendicular to the TOF axis, the mass peaks of I^+ and CH_3^+ ions have shoulder structures. It is known that the fragment CH_3^+ or I^+ is produced in the direction of the C–I bond, so the shoulder structures indicate that the CH_3I with the C–I bond perpendicular to the laser polarization also have substantial ionization-dissociation rates. This result is another evidence for the lack of dynamic alignment of CH_3I in the intense laser field.

B. Kinetic energy release and dissociation channels

With the high mass resolution of RTOF-MS, the fragment ions of same M mass number but from different dissociation channels can be all resolved clearly in the case of the parallel laser polarization shown in Fig. 2. The KER of the fragment ions can be calculated by the formula[22]

$$\mathrm{KER}\ (\mathrm{eV}) = 9.65 \times 10^{-7} \frac{\Delta t^2 q^2 F^2}{8M}, \tag{4}$$

where F is the static electric field ($F=168$ V/cm), q is the charge, M is the mass in amu of the fragment ions, and Δt represents the time difference in nanoseconds between the backward and forward components of the fragment ions from the same dissociation channel. The mass spectrum of typical fragment ions obtained with the parallel laser polarization in Fig. 2 is fitted by a sum of Gaussian distributions displayed in Fig. 3, and the KERs of the fragment ions calculated are listed in Table I. The above method with a Gaussian function has been applied to the case of the N_2 Coulomb explosion by Hishikawa *et al.*[33,34] and Nibarger *et al.*,[35] and is proved to be appropriate to represent the mixture of the contributions from the fragment ions. The H^+ ion peak in Fig. 2 is not well resolved because H^+ ions come from too many channels and the disturbance from water, so only a maximum KER of 11 eV is obtained. For H_2^+ ions, the maximum value of KER is about 8 eV. The KERs of I^{6+} and C^{3+} are calculated approximately from Fig. 1(a) without fitting.

In the following, we try to assign the dissociation channels by the high resolved mass spectrum as well as by the calculations. For this purpose, the ionization-dissociation of CH_3I is studied using different laser intensities, and the conservation of momentum and energy are used. The mark (p,q) is used to represent the two-body dissociation channel, $CH_3I^{n+} \rightarrow CH_3^{p+} + I^{q+}$ $(n=p+q)$. The detailed discussion is presented below.

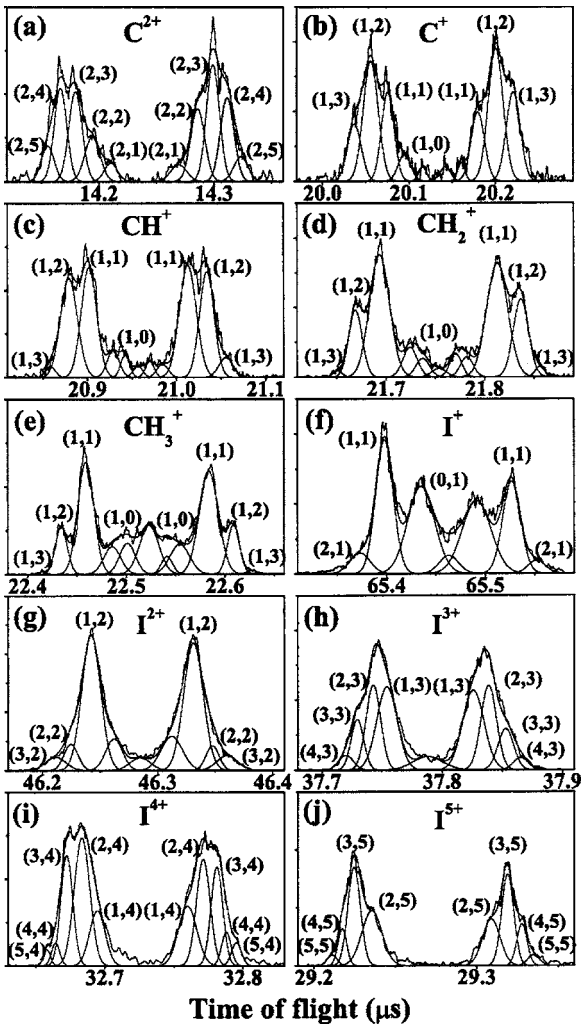

FIG. 3. Mass spectrum of typical fragment ion peaks fitted by a sum of Gaussian distributions with the identified (p,q). (a) C^{2+}, (b) C^+, (c) CH^+, (d) CH_2^+, (e) CH_3^+, (f) I^+, (g) I^{2+}, (h) I^{3+}, (i) I^{4+}, and (j) I^{5+}.

1. Multiphoton dissociation of CH_3I^+ ions

In Figs. 3(e) and 3(f), the CH_3^+ ions with KERs <1 eV are labeled (1,0) and I^+ ions with KER of 0.07 ± 0.03 eV are labeled (0,1). This assignment is done according to the following facts: (1) The KERs of CH_3^+ and I^+ are too small to assign from the Coulomb explosion of CH_3I^{n+}. (2) We studied the mass spectrum of the fragment ions of CH_3I recorded by a series of laser intensities attenuated successively about 10%, and we found that the KERs of the fragment ions were independent of laser intensities. For example, Fig. 4 records the mass spectrum at a laser intensity of 1.1×10^{14} W/cm^2 with laser polarization parallel to the TOF axis, and the KERs of channel (1,0) and (0,1) have the same profiles as the case of a laser intensity at 6.6×10^{14} W/cm^2 shown in Fig. 2. This character is consistent with the photon dissociation process where the KER of the fragments depends on the photon energy but is not influenced by laser intensity. So we suggest

TABLE I. The measured kinetic energy release of CH_3I in the intense laser field (6.6×10^{14} W/cm^2) determined by the Gaussian function fit of the mass spectrum. The assigned dissociated channels and the approximate R_c are also listed.

Dissociation channel (p,q)	R_c (Å)	KER (eV)											
		C^{3+}	C^{2+}	C^+	CH^+	CH_2^+	CH_3^+	I^{6+}	I^{5+}	I^{4+}	I^{3+}	I^{2+}	I^+
(1,0)/(0,1)				0.15	0.21	0.28	0.37						0.07
					0.78	0.82	0.91						
(1, 1)				3.06	3.22	3.44	3.60						0.43
(1, 2)	3.7			5.96	6.28	6.60	6.94					0.85	
(2, 1)	3.7		3.95										0.86
(1, 3)	3.7			9.56	10.0	10.2	10.5				1.25		
(2, 2)	3.8		9.60									1.62	
(1, 4)	3.4									1.81			
(2,3)/(3,2)	3.8		16.1								2.22	2.37	
(2, 4)	3.7		23.5							3.25			
(3, 3)	3.8										3.60		
(2, 5)	3.9		32.0						3.87				
(3,4)/(4,3)	3.7	36.6								5.0	4.91		
(3, 5)	3.8	42.5							6.04				
(4, 4)	3.7									6.59			
(3, 6)	3.5							7.78					
(4,5)/(5,4)	3.8								8.10	8.04			
(4, 6)	3.7							9.80					
(5, 5)	3.8								10.1				

that the fragment ions CH_3^+ and I^+ with low KERs are produced by multiphoton dissociation of CH_3I^+ ions. In early studies on CH_3I^+, it was reported that CH_3^+ was produced from the state $CH_3I^+(X\,^2E_{1/2})$ or the state $CH_3I^+(X\,^2E_{3/2})$ by absorbing a certain number of photons (higher than the barrier energy), while I^+ could be produced via the first excited state $CH_3I^+(\tilde{A})$ directly into I^+ and CH_3.[16,17] The reported dissociation channel and the needed dissociation energy (ΔE) are listed in Table II.

In our experiments, the 798 nm laser (about 1.55 eV) was used. From Table II the reported ΔE values are all higher than 1.55 eV, so CH_3I^+ needs to absorb two or three photons for dissociation. The KERs of dissociation fragments should be equal to the difference between the total photon energy and ΔE. The calculated KERs based on a multiphoton dissociation mechanism and the experimentally measured KERs for each channel are also listed in Table II. From Table II, we can see that the calculated KERs and the experimental KERs are in good agreement. For CH_3^+ ions, the middle peaks in Fig. 3(e) with very small KER of about 0.03 eV should be $CH_3I^+(X\,^2E_{1/2})+2h\nu\rightarrow CH_3^+ + I(^2P_{1/2})$, and the measured CH_3^+ with 0.36 eV is $CH_3I^+(X\,^2E_{3/2})+2h\nu\rightarrow CH_3^+ + I(^2P_{3/2})$. The CH_3^+ with 0.91 eV can be $CH_3I^+(X\,^2E_{1/2})+2h\nu\rightarrow CH_3^+ + I(^2P_{3/2})$ or $CH_3I^+(X\,^2E_{3/2})+3h\nu\rightarrow CH_3^+ + I(^2P_{1/2})$, which have similar KERs. For I^+ ions, as shown in Fig. 3(f), we only observed a pair of strong peaks at 0.07 eV, which can be assigned to $CH_3I^+(X\,^2E_{3/2})+3h\nu\rightarrow CH_3I^+(\tilde{A})\rightarrow CH_3+I^+(^3P_{1,0})$. The I^+ ions from other channels are too weak in mass spectrum and cannot be resolved. The I^+ ions have a wide energy range of KERs, from 0.04 to 0.1 eV, and the maximum value is 0.07 eV. The CH_3^+ ions have a broadened profile also in mass spectrum, similar to the case of I^+ ions. The broadened peak features of the fragment ions CH_3^+ and I^+, produced from multiphoton dissociation of CH_3I^+, are due to the frequency broadening of the femtosecond laser pulse, which makes CH_3^+ ions (or radical) present in many vibrational states.[16] The unmarked middle peak of I^+ ions in Fig. 3(f) might be a small contribution from perpendicular ionization-dissociation, so the middle peak of CH_3^+ ions in Fig. 3(e) also should be mixed with the contribution of CH_3^+ ions produced from perpendicular ionization-dissociation.

2. Coulomb explosion of CH_3I^{2+} and CH_3I^{3+} ions

The KERs of the fragment ions produced by the Coulomb explosion of CH_3I^{2+} or CH_3I^{3+} are much larger than those in the case of the CH_3I^+ dissociation. For the Coulomb explosion of CH_3I^{n+} ions, the KERs of the fragment ions are from the repulsive Coulomb force between the charged fragments. The KERs of the two fragments CH_3^{p+} and I^{q+} produced by the two-body dissociation channels have a relationship from the momentum conservation as follows:

$$\mathrm{KER}(I^{q+})/\mathrm{KER}(CH_3^{p+}) = M(CH_3^{p+})/M(I^{q+}), \tag{5}$$

where M is the mass of the fragment ions. Since the observed CH_3^+ ions can be from different precursors CH_3I^{q+} ($q=1,2,3$) by the two-body dissociation channels, so the CH_3^+ ions have different KERs, giving a distribution of CH_3^+ in mass spectrum. Using Eq. (5), for each CH_3^+ with the certain KER, the KER of the corresponding I^{q+} can be determined. For example, there are two groups of CH_3^+ ions in Fig. 3(e), and the CH_3^+ ions with 3.6 eV are assigned for channel (1,1). According to Eq. (5) the calculated KER of I^+ is 0.43 eV, which is in good agreement with the experimentally measured KER of I^+. Therefore, channel (1,1) with the exact total KER of 4.03 eV is identified. Similarly, the CH_3^+ ion with a KER of 6.94 eV is assigned for channel (1,2) and the corresponding I^{2+} ions have a KER of 0.84 eV labeled

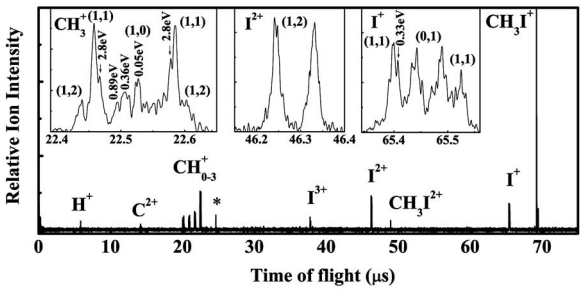

FIG. 4. Mass spectrum of CH_3I irradiated at a laser intensity of 1.1×10^{14} W/cm^2 with laser polarization parallel to the TOF axis.

(1,2) in Fig. 3(g). It is also found that the KERs of channel (1,1) and channel (1,2) are independent of the laser intensity. As shown in Fig. 4, at a laser intensity of 1.1×10^{14} W/cm^2, the measured KERs of CH_3^+ and I^+ ions from channel (1,1) are 3.6 and 0.43 eV, respectively, which are equal to the KERs measured at a laser intensity of 6.6×10^{14} W/cm^2.

The CH_3I^{2+} ions are observed in our experiments. The fact that some CH_3I^{2+} ions are still alive without Coulomb explosion indicates that there should be a bound potential well in CH_3I^{2+} ions near R_e, the equilibrium C–I internuclear distance of CH_3I, to avert Coulomb explosion.[2] So the KER of the fragments CH_3^+ and I^+ from the CH_3I^{2+} cannot be simply calculated by a Coulomb repulsion between CH_3^+ and I^+ at the equilibrium C–I internuclear distance. The contribution of the potential well makes the KERs lower than those from an ordinary Coulomb explosion. If it is supposed that one of the charges is on I atom and the other is on C atom, the Coulomb repulsion energy can be approximated by $E_{1,1}$ (eV)$=14.4/R_e$, which is from the common formula of the Coulomb repulsion energy of $CH_3^{p+}I^{q+}$ at $R_e=2.14$ Å as follows:

$$E_{p,q}\ (\mathrm{eV}) = 14.4\frac{pq}{R_e}, \tag{6}$$

where p and q are the charges of the two fragments, R_e is the equilibrium C–I internuclear distance of CH_3I in angstrom and $E_{p,q}$ is the total KER of the given channel (p,q). By Eq. (6) the calculated $E_{1,1}$ is about 6.73 eV, which is higher than the measured total energy of 4.03 eV. The fact that the measured total KER of channel (1,1) is lower than the value calculated from Eq. (6) signifies the presence of the metastable state in CH_3I^{2+} and the contribution of the covalent forces.

Another group of CH_3^+ ions with KER of 2.8 eV is observed in Fig. 4, and the corresponding I^+ ions with 0.33 eV are also found in Fig. 4. The total KER is 3.13 eV. The two dissociation channels with KER 4.03 and 3.13 eV are explained respectively as follows:

$$CH_3I^{2+} \rightarrow CH_3^+ + I^+(^3P_2) \quad (4.03\ \text{eV KERs}), \tag{7a}$$

$$CH_3I^{2+} \rightarrow CH_3^+ + I^+(^3P_{1.0}) \quad (3.13\ \text{eV KERs}). \tag{7b}$$

For channel (1,2), the parent precursor CH_3I^{3+} ions have not been observed in the experiments. This fact indicates that as the number of removed electrons increases, the Coulomb repulsion becomes much stronger than the binding forces, and the fragment ions from precursor CH_3I^{3+} are produced by the Coulomb explosion. However, the measurements show that the total KER of channel (1,2), 7.78 eV, is much lower than the $E_{1,2}=13.46$ eV calculated by Eq. (6). The energy deficit of channel (1,2) is 5.68 eV (13.46−7.78 eV) larger than that of channel (1,1), 2.7 eV (6.73−4.03 eV). The result seems to be conflicting with the fact that as removed electrons increase, the contribution of the remaining valence forces is decreased and the KER should be close to the Coulomb energy. This problem might be solved by replacing R_e with R_c in Eq. (6). R_c is the valid distance of the two point charges separated in the two parts of the fragments before explosion. It can be easily understood that during the ionization of CH_3I^{2+} to CH_3I^{3+}, the nuclei (C and I) have time to move apart from each other. So the Coulomb energy should be calculated using the valid R_c instead of R_e. The truth might be that the charges are not simply located on carbon atom, but are distributed on the whole CH_3 group. The use of R_c just represents the valid distance between these two point charges. Using the measured total KER 7.78 eV

TABLE II. The calculated KERs based on mutiphoton dissociation channels of CH_3I^+, and comparison with the measured KERs from the experiments.

			KER (eV)			
Dissociation channels of CH_3I^+	ΔE	$h\upsilon$	I^+ or CH_3^+ (Calc.)		I^+ or CH_3^+ (Expt.)	
$CH_3I^+(X\,^2E_{1/2}) \rightarrow CH_3^+ + I(^2P_{3/2})$	2.1	2	CH_3^+	0.89	CH_3^+	0.91
$CH_3I^+(X\,^2E_{3/2}) \rightarrow CH_3^+ + I(^2P_{3/2})$	2.73	2	CH_3^+	0.36	CH_3^+	0.37
$CH_3I^+(X\,^2E_{1/2}) \rightarrow CH_3^+ + I(^2P_{1/2})$	3.04	2	CH_3^+	0.05	CH_3^+	0–0.03
$CH_3I^+(X\,^2E_{3/2}) \rightarrow CH_3^+ + I(^2P_{1/2})$	3.67	3	CH_3^+	0.88	CH_3^+	0.91
$CH_3I^+(X\,^2E_{1/2}) \rightarrow CH_3I^+(\tilde{A})$ $\rightarrow CH_3 + I^+(^3P_2)$	2.7	2	I^+	0.05	I^+	
$CH_3I^+(X\,^2E_{3/2}) \rightarrow CH_3I^+(\tilde{A})$ $\rightarrow CH_3 + I^+(^3P_2)$	3.33	3	I^+	0.14	I^+	
$CH_3I^+(X\,^2E_{1/2}) \rightarrow CH_3I^+(\tilde{A})$ $\rightarrow CH_3 + I^+(^3P_{1,0})$	3.54	3	I^+	0.11	I^+	
$CH_3I^+(X\,^2E_{3/2}) \rightarrow CH_3I^+(\tilde{A})$ $CH_3 + I^+(^3P_{1,0})$	4.17	3	I^+	0.07	I^+	0.07±0.03

and ignoring any initial energies, we can calculate approximately the R_c of channel (1,2) using Eq. (6) to be about 3.7 Å.

The R_c defined here (the valid interdistance between two point charges) is somewhat different from the case of diatomic molecules.[1] For diatomic molecules, R_c is generally considered as the internuclear distance between the two nuclei, at which enhanced ionization proceeds and Coulomb explosion occurs.[8] The generation of the enhanced ionization at R_c explains why KERs of fragment ions are actually independent of laser intensity and wavelength.[4] In the case of methyl iodide, the enhanced ionization to produce CH_3I^{3+} in the intense laser field is also considered to occur at R_c as above because the KER of channel (1,2) is independent of laser intensity. For example, with a laser intensity of 1.1×10^{14} W/cm^2, the measured KER of channel (1,2) is about 7.7 eV, and with a laser intensity 6.6×10^{14} W/cm^2 the measured KER is 7.78 eV. The result is considered as an evidence that the enhanced ionization of methyl iodide in the intense laser field happens at $R_c\approx3.7$ Å.

Figure 3(f) depicts the distribution of I^+ ions in mass spectrum. It can be resolved that one group of I^+ ions has a KER of 0.86 eV. Using Eq. (5), the calculated KER of the corresponding CH_3^{p+} is about 7.3 eV, which is very close to the CH_3^+ ions with 6.94 eV. If I^+ with 0.86 eV and CH_3^+ ions with 6.94 eV is a pair of ions, the two kinds of fragment ions should be present together in mass spectrum. But the I^+ ions with 0.86 eV are not present in some mass spectra, while the CH_3^+ ions with 6.94 eV are present. So the CH_3^+ ions with 6.94 eV are assigned for channel (1,2) to produce I^{2+} with a KER of 0.85 eV. For example, with a laser intensity of 1.1×10^{14} W/cm^2, there are no I^+ ions with 0.86 eV, but the CH_3^+ ion with 6.94 eV and I^{2+} with 0.84 eV still coexist. We suggest that the I^+ ions with 0.86 eV is from other dissociation channels of CH_3I^{3+}, either the sequential two-body channel $CH_3I^{3+}\rightarrow CH_3^{2+}+I^+$ followed by $CH_3^{2+}\rightarrow H^++CH_2^+$ or the nonsequential three body fragment channel $CH_3I^{3+}\rightarrow H^++CH_2^++I^+$. It is difficult to distinguish experimentally between the two channels because for the (2,1) channel, the intermediate CH_3^{2+} is not observed due to dissociation into the final products CH_2^+ and H^+. This means that the sequential and nonsequential channels give the same final products. The sequential and nonsequential channels represent the two limiting cases of fragmentation behaviors, and other physical processes are also possible to occur; e.g., a stretching of C–I bond is followed by a rapid dissociation of the C–H bond. Anyway, the detailed confirmation cannot be obtained by present experiments. In Fig. 3 for $p\geqslant2$, we use (p,q) just to represent the main two-body dissociation channels with the proposed possible total charge numbers without concerning the detailed mechanisms. So I^+ ion with 0.86 eV is labeled (2,1) in Fig. 3(f) The determination of the (p,q) with a given I^{q+} is discussed in Sec. III B 4.

3. Stepwise dissociation of CH_3^+ ion

The mass spectrum in Fig. 3 shows that the fragment CH_3^+ ions have different KERs, indicating that the CH_3^+ ions come from different ionization-dissociation channels, as marked by (1,0), (1,1), (1,2), and (1,3). The CH_3^+ ions from different channels correspond to different groups of fragment ions CH_m^+ $(m=0-2)$, which have KER close to that of the corresponding CH_3^+. For example, as shown in Table I, the CH_3^+ from channel (1,1) has a KER of 3.60 eV, and the corresponding CH_m^+: KERs of 3.06 eV C^+, 3.22 eV CH^+, and 3.44 eV CH_2^+. The KERs of CH_m^+ are found to be independent of the laser intensity, which could be an evidence that CH_m^+ are produced from the stepwise dissociation of CH_3^+ ions. After the primary dissociation, some of the CH_3^+ ions can stepwise dissociate to smaller fragment ions by dropping H atoms. The possible dissociation channels are expressed as follows:

$$CH_3^+\rightarrow CH_2^++H, \tag{8a}$$

$$CH_2^+\rightarrow CH^++H, \tag{8b}$$

$$CH^+\rightarrow C^++H. \tag{8c}$$

In channels (8a)–(8c) each of the dropped H atoms can carry away a small part of kinetic energy from the parent precursors. So the following order of the KERs resulted: $KER(C^+)<KER(CH^+)<KER(CH_2^+)<KER(CH_3^+)$. The experimentally measured KERs of CH_m^+ listed in Table I show clearly this tendency. For channel (1,0), the CH_3^+ ions with 0.36 eV are stepwise dissociated to CH_2^+ ions with 0.28 eV and CH^+ ions with 0.21 eV, while the CH_3^+ ions with 0.91 eV are stepwise dissociated to CH_2^+ ions with 0.82 eV and CH^+ ions with 0.78 eV. The C^+ ions produced from CH_3^+ ions of channel (1,0) with lower KER are not clearly resolved due to their very weak signals. All the fragment ions, CH_m^+ $(m=0-3)$, $CH_3I^+\rightarrow CH_3^++I$, i.e., (1,0), are labeled (1,0) in Figs. 3(b)–3(d). For the fragment ions of CH_3^+ ions with 3.6 eV from channel (1,1), the corresponding CH_2^+ ions with 3.44 eV, CH^+ ions with 3.22 eV, and C^+ ions with 3.06 eV are all labeled (1,1) in Figs. 3(b)–3(d), while the split from the coupling of the spin-orbit energy of I^+ via Eq. (7b) is not resolved. For the fragment ions of CH_3^+ ions with 6.94 eV from channel (1,2), the corresponding CH_2^+ ions with 6.6 eV, CH^+ ions with 6.28 eV, and C^+ ions with 5.96 eV are all labeled (1,2) in Figs. 3(b)–3(d).

In the stepwise dissociation of CH_3^+, it is shown that the KER difference between CH_m^+ and CH_{m-1}^+ ions in the same channel increases as the KER of parent CH_3^+ increases. This can be explained by the fact that the energy carried away from CH_3^+ by the H atom is directly proportional to the total energy of the parent precursor CH_3^+ from the conservation of energy and momentum. For example, for the CH_3^+ with a KER of 3.6 eV from channel (1,1), the KER of CH_2^+ is about 3.44 eV with the difference, $3.6-3.44=0.16$ eV, which is less than $6.94\ (CH_3^+)-6.6\ (CH_2^+)=0.34$ eV from channel (1,2). The experiments also show that the CH_3^+ ions with higher KER are more easily dissociated into fragments. For example, as shown in Fig. 3(e), the relative abundance of CH_3^+ ions from channel (1,1) is larger than twice of CH_3^+ ions from channel (1,2), but the relative abundances of CH_m^+ ions from channel (1,2) increase prominently in Figs. 3(b)–3(d), and especially the abundance of C^+ ions from channel (1,2)

is about twice that of channel (1,1). This fact is explained that with higher KER, the CH_3^+ ions will have higher internal energy, which leads to CH_3^+ ions more active and easily dissociated.

4. Coulomb explosion of CH_3I^{n+} ions with $n \geq 4$

For the Coulomb explosion of the highly charged CH_3I^{n+} precursors with $n \geq 4$, only I^{q+} ions are identified in the mass spectrum. The KERs of I^{q+} are measured and listed in Table I. The CH_3^{p+} ions with $p > 1$ are not obtained because they are unstable and further dissociated into the smaller fragment ions. For this reason it is difficult experimentally to identify Coulomb explosion channels of higher charged CH_3I^{n+} as well as their total KER. For this purpose the following mode is supposed.

The charge distribution on the whole methyl can be considered as a point charge p, while the charge distribution on the I atom can be considered as another point charge q. The interdistance between the two point charges p and q is denoted as R_c. With the supposition, the KERs of the CH_3^{p+} and I^{q+} can be obtained from the Coulomb repulsion between CH_3^{p+} and I^{q+} with the distance R_c by Eq. (6). The $R_c \approx 3.7$ Å has been calculated for CH_3I^{3+}, and this value of R_c can be extended to all the Coulomb explosion of CH_3I^{n+}; i.e., the value around 3.7 Å is the virtual distance between CH_3^{p+} and I^{q+}. According to the conservation of momentum and energy, from the known KER of the I^{q+}, the total KER of $CH_3^{p+}I^{q+}$ can be obtained by

$$E_{p,q} \approx 142 \times \mathrm{KER}(I^{q+})/15. \quad (9)$$

Using the $R_c = 3.7$ Å, for each I^{q+} peak, the corresponding charge p of the CH_3 group can be estimated by Eq. (6). For example, the total KER of the channel with 1.62 eV of I^{2+} can be calculated, $E_{p,2} = 142 \times 1.62/15 = 15.34$ eV. Then we get $p = 1.97 \approx 2$ from Eq. (6). Therefore, channel (2,2) with KER of I^{2+}, 1.62 eV, is identified. Thus all the I^{q+} ions with different KERs are identified and labeled in Fig. 3.

It is noticed that channel (1,3) with KER 10.5 eV of CH_3^+ and 1.25 eV of I^{3+} is identified by the very weak CH_3^+ signal. The fact that the CH_3^+ with 10.5 eV is very weak is coincident with the fact that the CH_3^+ with large KER is easily dissociated into small fragments, CH_m^+ $(m=0-2)$. In Figs. 3(b)–3(d), the CH_m^+ peaks from channel (1,3) can be clearly identified, and the abundance is increased with the decrease of H atoms. However, for channel (1,4), only partially resolved I^{4+} and the corresponding series of CH_m^+ are not observed in Fig. 3. In Fig. 3(g), another I^{2+} peak with a KER of 0.3 eV is identified, but the corresponding CH_m^{p+} ions are not found. This KER value of I^{2+} is close to that of I^+ from channel (1,1), so I^{2+} ions with 0.3 eV are supposed to be from further ionization of I^+ ions.

The C^{2+} ions and C^{3+} ions are assigned as the final products of CH_3I^{n+}, corresponding to I^{q+} ions with higher charges. The assignment can be demonstrated by the experiments attenuating laser intensity. For example, Fig. 5 shows the mass spectrum of the fragment ions of CH_3I irradiated by the laser intensity of 7.7×10^{13} W/cm^2 with laser polarization parallel to the TOF axis. It can be seen that C^{2+} and C^{3+} ion peaks, and the I^{q+} $(q \geq 3)$ disappear simultaneously. So

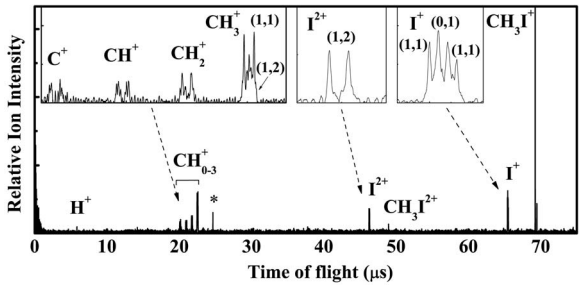

FIG. 5. Mass spectrum of CH_3I irradiated at a laser intensity of 7.7×10^{13} W/cm^2 with laser polarization parallel to the TOF axis.

the C^{2+} ions or C^{3+} ions are only observed with the observation of I^{q+} $(q \geq 3)$. By the experiments with a series of laser intensities, we find that C^{3+} is correlated to I^{5+} and I^{4+}, and that C^{2+} is correlated to I^{4+} and I^{3+}. The detailed dissociation mechanism is still unclear.

C. The charge distributions for the Coulomb explosion of methyl iodide

As shown in Table I and Fig. 3, the parent precursor ions of the same number of charges can have different charge distributions and can be dissociated into different fragment ions. The even charged methyl iodide has two dissociation patterns. One is the symmetric channel with $p=q$, and the other is the asymmetric channel with $p+2=q$. The fragment ions CH_3^{p+} and I^{q+} with $p > q$ produced from the Coulomb explosion of the even charged methyl iodide are not observed. For the same parent precursor ions, we calculated the ion abundance for each channel and found that the fragment ion abundance of the asymmetric channel was larger than that of the symmetric channel. The odd charged methyl iodide has two dissociation patterns. One pattern includes two series, $p=q+1$ and $p=q-1$ $(p+q=n)$ with similar total KERs, and another pattern is $p+3=q$. For a given charged parent precursor, the series of channels $(q+1,q)$ are the minor channels because their ion peaks are very weak, as shown in Fig. 3, and the series of channels $(q-1,q)$ are the dominant channels with very strong ion peaks. The ion abundance of the channel with $p+3=q$ is a little smaller than that of channel $(q-1,q)$. All the above results indicate that in the intense laser field, electron can be detached more easily from iodine atom than from methyl radical, so the charge on iodine atom is higher than that on methyl radical in most cases.

IV. CONCLUSION

The dissociation of CH_3I^+ is concluded by multiphoton dissociation mechanism, in which the excited state of CH_3I^+ is produced by absorbing two or three photons and then the dissociation occurs through channel (1,0) to produce CH_3^+ ions or through channel (0,1) to produce I^+. The calculated KERs of CH_3^+ and I^+ based on multiphoton dissociation mechanism agree well with the measured values in experiments. The CH_3I^{2+} ions were observed in experiments, and their dissociation to produce CH_3^+ and I^+ is also observed in mass spectrum. But the measured KERs of CH_3^+ and I^+ produced from CH_3I^{2+} are much lower than the calculated ones

by the Coulomb explosion, which is explained by the existence of a bound potential well near R_e of C–I for CH_3I^{2+}. Two groups of fragment ions CH_3^+ and I^+ from CH_3I^{2+} are observed, and they have total KERs of 4.03 and 3.13 eV, respectively. It is suggested that the difference is caused by the energy splitting of $I^+(^3P_2)$ and $I^+(^3P_{0,1})$.

By the measurement of the KER of channel (1,2) the R_c is introduced to explain the energy deficit of CH_3I^{3+}. Here the R_c is defined ($R_c \approx 3.7$ Å) as the valid charge distance (~ 3.7 Å) between I^{2+} and CH_3^+, at which enhanced ionization of methyl iodide happens. The fragments CH_m^+ ($m=0-2$) in mass spectrum are considered as the stepwise dissociation of CH_3^+. The dissociation rate is increased with the KER increase of CH_3^+. For the Coulomb explosion of CH_3I^{n+} with $n \geqslant 4$, it is difficult experimentally to distinguish the sequential two-body charge separation or nonsequential multiple fragmentation due to the lack of CH_3^{p+} ($p \geqslant 2$) ions in mass spectrum. For I^{q+} ($q \geqslant 3$) observed in mass spectra, the Coulomb repulsion model with two point charges p and q at distance $R_c \approx 3.7$ Å is used to calculate the corresponding charge p of CH_3^{p+}. The correlations of final products C^{2+} and C^{3+} with I^{q+} ($q \geqslant 3$) are examined by laser intensity experiments. Finally, the charge distribution in the dissociation of CH_3I^{n+} is discussed. By comparing the mass abundance of fragment ions, it is found that charge asymmetric dissociation channels with $p < q$ (i.e., more charges on the iodine atom) are the dominant channels.

ACKNOWLEDGMENTS

The experimental results in this paper are obtained in Institute of Chemistry, Chinese Academy of Sciences. The authors gratefully acknowledge the support of the National Natural Science Foundation of China under Grant Nos. 20203020 and 20433080. They also thank Professor Qihe Zhu and Professor Fanao Kong for their helpful discussion.

[1] K. Codling and L. J. Frasinski, J. Phys. B **26**, 783 (1993).
[2] J. H. Posthumus and J. F. McCann, *Molecules and Clusters in Intense Laser Fields*, edited by J. H. Posthumus (Cambridge University Press, Cambridge, UK, 2001).
[3] R. J. Levis and M. J. DeWitt, J. Phys. Chem. A **103**, 6493 (1999).
[4] J. H. Posthumus, Rep. Prog. Phys. **67**, 623 (2004).
[5] H. Stapelfeldt and T. Seideman, Rev. Mod. Phys. **75**, 543 (2003).
[6] H. Niikura, F. Legare, R. Hasbani, A. D. Bandrauk, M. Y. Ivanov, D. M. Villeneuve, and P. B. Corkum, Nature (London) **417**, 917 (2002).
[7] G. N. Gibson, M. Li, C. Guo, and J. P. Nibarger, Phys. Rev. A **58**, 4723 (1998).
[8] J. H. Posthumus, A. J. Giles, M. Thompson, W. Shaikh, A. J. Langley, L. J. Frasinski, and K. Codling, J. Phys. B **29**, L525 (1996).
[9] J. H. Posthumus, L. J. Frasinski, A. J. Giles, and K. Codling, J. Phys. B **28**, L349 (1995).
[10] M. Plummer and J. F. McCann, J. Phys. B **29**, 4625 (1996).
[11] T. Seideman, M. Y. Ivanov, and P. B. Corkum, Phys. Rev. Lett. **75**, 2819 (1995).
[12] D. Pavicic, A. Kiess, T. W. Hansch, and H. Figger, Phys. Rev. Lett. **94**, 163002 (2005).
[13] C. Kosmidis, P. Siozos, S. Kaziannis, L. Robson, K. W. D. Ledingham, P. McKenna, and D. A. Jaroszynski, J. Phys. Chem. A **109**, 1279 (2005).
[14] D. M. Szaflarski and M. A. El-Sayed, J. Phys. Chem. **92**, 2234 (1988).
[15] L. Lehr, R. Weinkauf, and E. W. Schlag, Int. J. Mass. Spectrom. **206**, 191 (2001).
[16] K. Walter, R. Weinkauf, U. Boesl, and E. W. Schlag, J. Chem. Phys. **89**, 1914 (1988).
[17] P. Sharma, R. K. Vatsa, B. N. Rajasekhar, N. C. Das, T. K. Ghanty, and S. K. Kulshreshtha, Rapid Commun. Mass Spectrom. **19**, 1522 (2005).
[18] B. L. Zhang, X. Y. Wang, N. Q. Lou, B. Zhang, and J. Wei, Spectrochim. Acta, Part A **57**, 1759 (2001).
[19] D. P. Zhong, P. Y. Cheng, and A. H. Zewail, J. Chem. Phys. **105**, 7864 (1996).
[20] D. P. Zhong and A. H. Zewail, J. Phys. Chem. A **102**, 4031 (1998).
[21] P. Graham, K. W. D. Ledingham, R. P. Singhai, S. M. Hankin, T. McCanny, X. Fang, C. Kosmidis, P. Tzallas, P. F. Taday, and A. J. Langley, J. Phys. B **34**, 4015 (2001).
[22] P. Siozos, S. Kaziannis, and C. Kosmidis, Int. J. Mass. Spectrom. **225**, 249 (2003).
[23] S. Kaziannis, P. Siozos, and C. Kosmidis, Chem. Phys. Lett. **401**, 115 (2005).
[24] R. Ma, C. Y. Wu, N. Xu, J. Huang, H. Yang, and Q. H. Gong, Chem. Phys. Lett. **415**, 58 (2005).
[25] J. H. Posthumus, J. Plumridge, M. K. Thomas, K. Codling, L. J. Frasinski, A. J. Langley, and P. F. Taday, J. Phys. B **31**, L553 (1998).
[26] S. Augst, D. Strickland, D. D. Meyerhofer, S. L. Chin, and J. H. Eberly, Phys. Rev. Lett. **63**, 2212 (1989).
[27] S. Larochelle, A. Talebpour, and S. L. Chin, J. Phys. B **31**, 1201 (1998).
[28] X. P. Xing, Z. X. Tian, P. Liu, Z. Gao, Q. Zhu, and Z. C. Tang, Chin. J. Chem. Phys. **15**, 83 (2002).
[29] X. P. Xing, Z. X. Tian, H. T. Liu, and Z. C. Tang, J. Phys. Chem. A **107**, 8484 (2003).
[30] C. Cornaggia, Phys. Rev. A **52**, R4328 (1995).
[31] C. Cornaggia, Phys. Rev. A **54**, R2555 (1996).
[32] C. Ellert and P. B. Corkum, Phys. Rev. A **59**, R3170 (1999).
[33] A. Hishikawa, A. Iwamae, K. Hoshina, M. Kono, and K. Yamanouchi, Chem. Phys. Lett. **282**, 283 (1998).
[34] A. Hishikawa, A. Iwamae, K. Hoshina, M. Kono, and K. Yamanouchi, Chem. Phys. **231**, 315 (1998).
[35] J. P. Nibarger, S. V. Menon, and G. N. Gibson, Phys. Rev. A **63**, 053406 (2001).